Direct Detection of Dark Asteroid

Anirban Das

E-mail: anirband@slac.stanford.edu
SLAC National Accelerator Laboratory, 2575 Sand Hill Road, Menlo Park, CA 94025, USA

Sebastian A. R. Ellis

E-mail: sarellis@protonmail.com
Institut de Physique Théorique, Université Paris Saclay, CEA, F-91191 Gif-sur-Yvette, France

Philip C. Schuster

E-mail: schuster@slac.stanford.edu
SLAC National Accelerator Laboratory, 2575 Sand Hill Road, Menlo Park, CA 94025, USA

Kevin Zhou

E-mail: knzhou@stanford.edu
SLAC National Accelerator Laboratory, 2575 Sand Hill Road, Menlo Park, CA 94025, USA

Abstract. Macroscopic dark matter is almost unconstrained over a wide "asteroid-like" mass range, where it could scatter on baryonic matter with geometric cross section. We show that when such an object travels through a star, it produces shock waves which reach the stellar surface, leading to a distinctive transient optical, UV and X-ray emission. This signature can be searched for on a variety of stellar types and locations. In a dense globular cluster, such events occur far more often than flare backgrounds, and an existing UV telescope could probe orders of magnitude in dark matter mass in one week of dedicated observation.

Dark matter (DM) could be in the form of objects of macroscopic mass and size, a possibility which is consistent with all cosmological constraints [1, 2, 3]. While macroscopic DM arises in many theoretical scenarios, it is difficult to detect terrestrially primarily because such objects are rare, given the low local DM density. As $M_{\rm DM}$ increases, experimental searches require either large detection volumes or long integration times.

In this work, we point out that because dark asteroids move supersonically in stars, dissipation through any non-gravitational interaction will generate shock waves. This allows the dissipated energy to quickly propagate to the stellar surface, where it is released in the form of a transient, thermal ultraviolet (UV) emission. Crucially, such events are correlated with the local DM density, but uncorrelated with the underlying activity of the star. Next-generation survey telescopes would detect such events without requiring a dedicated search, while existing telescopes could find them by monitoring regions of high DM density. This would constitute a DM direct detection experiment on astronomical scales, with the stars as the detector volume.

We will introduce our signature by assuming that all DM is in the form of spherical dark asteroids with the same mass $M_{\rm DM}$ and radius $R_{\rm DM}$. We further assume that they scatter baryons elastically with geometric cross section $\sigma = \pi R_{\rm DM}^2$, enter the star head-on, and do not disintegrate while passing through the star. In the final section, we discuss how these properties can arise and how the signature changes when they are relaxed.

Stellar collisions.—We compute stellar profiles with MESA [4], assuming solar metallicity and the settings recommended by MIST [5], and match them at the photosphere to atmospheric profiles computed with PHOENIX [6]. When a dark asteroid enters a star of mass $M_\star$ and radius $R_\star$, it will be traveling at roughly the escape velocity $v_{\rm esc} = \sqrt{2GM_\star/R_\star}$, and is therefore hypersonic, with Mach number $\mathrm{Ma} \sim 100$. It is accelerated inward by gravity, and dissipates energy due to a drag force $\rho\sigma v^2 c_d/2$, where $c_d \simeq 1$ for a supersonic sphere. For most of the parameters we consider, the dark asteroid remains hypersonic until it either dissipates most of its energy to drag, or reaches the hot stellar core.

Describing the resulting production and propagation of shock waves is a complex hydrodynamic problem. However, it can be decomposed into simpler problems each solvable by controlled approximations. First, because the dark asteroid is hypersonic, $\mathrm{Ma} \gg 1$, its passage can be treated as an instantaneous deposition of energy $F_{\rm dr}$ per unit length, which creates a cylindrical blast wave. The shock wave becomes weak after it travels a characteristic radial distance $R_0 = \sqrt{2F_{\rm dr}/p} \sim \mathrm{Ma}\, R_{\rm DM}$, and asymptotically approaches an N-wave profile, a weak shock solution characterized by a pressure discontinuity Δp and length L. Following Ref. [7], we match a blast wave onto an N-wave profile at distance $10R_0$, where the shock strength is $\Delta p/p = 0.06$, the length is $L = 2.8R_0$, and roughly half of the original energy remains in the shock wave.

To treat the propagation to the stellar surface, we use standard results from weak shock theory [8]. In particular, the propagation of a weak shock wave through a slowly varying medium can be described by geometric acoustics. Because the speed of sound decreases with distance from the center of the star, the ray paths refract radially outward. We propagate each piece of the shock front along such a ray. For an acoustic wave, if the wavefront area evolves as $A(s)$ along a ray, then the pressure amplitude varies as $\Delta p \propto \sqrt{\rho c_s/A(s)}$, while the period L/c_s remains constant. The discontinuities of an N-wave cause additional dissipation: when the shock wave travels a length L, there is a fractional increase in L, and a fractional decrease in shock strength and total energy, of order $\Delta p/p$.

Finally, as each piece of the shock front approaches the stellar surface, the decreasing density and pressure cause a rapid increase in the shock strength. Analytic solutions exist to describe the arrival of a strong shock wave at the edge of a star. To roughly approximate these results, we assume that once the shock wave becomes strong, $\Delta p/p \gtrsim 1$, its remaining energy heats the stellar material above it to a uniform temperature T_f, which sets the typical frequency band of emission. This is reasonable because convection near the stellar surface will effectively smooth out temperature gradients as energy is radiated from the surface. The timescale for energy release is then dictated by the rate of blackbody radiation, and is typically on the order of hundreds of seconds.

In Fig. 1, we show the total shock energy released from the surface of a Sun-like star, and the typical final temperature T_f. The qualitative features of this plot can be readily understood. For higher $R_{\rm DM}$, the dark asteroid stops near the stellar surface, and a small portion of the surface is heated to a high temperature. As $R_{\rm DM}$ decreases, the shock waves are primarily produced deeper in the star, with a shorter wavelength. This increases the dissipation they experience as they propagate out to the surface, decreasing the energy released. At the smallest radii, drag is insufficient to prevent the dark asteroid from passing through the entire star, so that only part of its energy is deposited, leading to a rapid fall-off in signal energy.

Since a strong shock has $\Delta T/T \sim 1$, the temperature T_f roughly tracks the local temperature at the depth where the weak shock becomes strong again; as a result, it is relatively insensitive

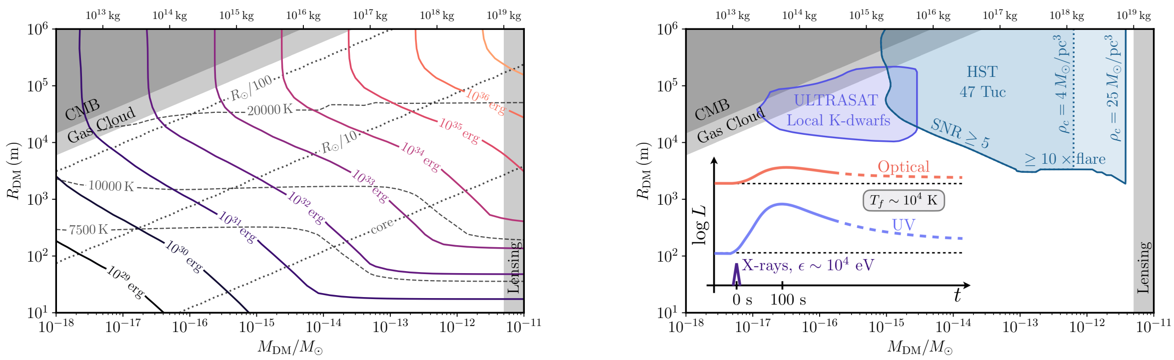

Figure 1. (Left) Contours of energy release (solid), characteristic temperature (dashed), and penetration depth (dotted) for a dark asteroid impact on a Sun-like star. We show bounds from the CMB limit on DM-baryon scattering [9], heating of cold gas clouds [10], and microlensing [11]. (Right) Contour plot showing observability. We shade regions where impacts on K dwarfs within 1 kpc would be seen by ULTRASAT, and impacts on Sun-like stars in 47 Tuc would be seen by HST, at least once per year and week of observation on average, respectively. For 47 Tuc, we show two possible values of the core DM density, as discussed in the main text, and require the rate of dark asteroid impacts to exceed superflares of similar energy by at least an order of magnitude. A schematic light curve for three frequency bands is shown in the inset.

to $M_{\rm DM}$ and $R_{\rm DM}$, and typically peaks in the far UV. At lower densities, T_f rapidly rises because the dark asteroid stops so close to the surface that the shock never becomes weak. At the very lowest densities shown, the dark asteroid stops above the photosphere. In this extreme case, the emission spectrum is not necessarily thermal, and depends on the detailed physics of the resulting plasma.

Observational prospects.—Dark asteroids are expected to produce rare transients on all types of stars, with a frequency dependent on the stellar and local DM parameters. For a star moving with a DM halo, averaging over a Maxwellian velocity distribution for the DM yields a collision rate [12]

$$\Gamma = \sqrt{\frac{8}{3\pi}}\frac{\rho_{\rm DM} v_d}{M_{\rm DM}}\,\pi R_\star^2 \left(1 + \frac{3v_{\rm esc}^2}{2v_d^2}\right) \tag{1}$$

where v_d is the velocity dispersion. The final term accounts for the focusing effect of gravitational attraction. In all cases we will consider, $v_{\rm esc} \gg v_d$, giving

$$\Gamma \simeq (4\times 10^{-5}\,{\rm yr}^{-1})\,\frac{M_\star}{M_\odot}\frac{R_\star}{R_\odot}\times\frac{10^{-15}M_\odot}{M_{\rm DM}}\,\frac{\rho_{\rm DM}}{0.4\,{\rm GeV/cm^3}}\,\frac{270\,{\rm km/s}}{v_d}. \tag{2}$$

As shown in the inset of figure 1, we expect a brief X-ray emission as the dark asteroid passes through the stellar atmosphere, followed by a gradual optical and UV emission as the shock wave produced inside reaches the surface of the star. Since most of the energy emerges in the UV, and cooler stars emit relatively little in this band, it is easiest to search for these events as UV transients.

The light curve would also have a long tail as the violently heated patch of the stellar surface gradually cools, which could be targeted for follow-up optical observation. Note that we have treated all collisions as head-on, though the high degree of gravitational focusing implies that most collisions are glancing. Our calculation is thus maximally conservative, because it gives the shock waves the longest possible path to the surface.

Upcoming transient surveys could detect dark asteroid collisions on nearby stars without requiring a dedicated search. Among star types, K dwarfs are promising targets, as they have significantly larger masses and radii than M dwarfs, but also have a higher number density and negligible UV emission compared to hotter stars. As a concrete example, we consider ULTRASAT [13], a proposed wide-field UV transient explorer designed to detect distant supernova shock breakouts, which will also monitor many nearby stars. We compute the maximum distance from which ULTRASAT could observe dark asteroid collisions at SNR ≥ 5, conservatively counting only impacts on K dwarfs, and approximate the star density as uniform out to 1 kpc from the Earth. The observable region of parameter space is cut off at high $R_{\rm DM}$ because the signal temperature becomes too high, at low $R_{\rm DM}$ and $M_{\rm DM}$ because the signal energy becomes too low, and at high $M_{\rm DM}$ because the events become too rare.

A similar region could be probed by the upcoming LSST survey [14], but estimating the event rate is more difficult because of LSST's complex observing strategy and multiple filters. In addition, since LSST would be able to see events at a significantly larger distance $d \gtrsim$ kpc, a more detailed model of the galactic stellar and DM densities would be required, along with estimates of UV extinction.

An alternative strategy is to perform a focused search in a region where the impact rate per star is significantly higher, such as the globuler cluster 47 Tuc (NGC 104) which has a dense core and negligible UV dust extinction.

While the DM content of globular clusters today is not known [15, 16], they are thought to have formed in large DM subhalos [17, 18], with computational studies suggesting an initial DM mass of about 260 times the stellar mass [19]. Tidal stripping and DM thermalization are expected to have reduced the DM content of the globular cluster since formation [20], with $\sim$1% remaining today [21]. We assume this formation history holds for 47 Tuc, and model the DM distribution with an NFW profile [22].

We infer a core DM density $\rho_{\rm DM} \simeq 4\, M_\odot/{\rm pc}^3$. Since the velocity dispersion is $v_d \simeq 12\,{\rm km/s}$, the collision rate per star is almost 4 orders of magnitude higher than in the local region, even though DM is still a vastly subdominant component of the core. For most of the parameters we consider, the event rate exceeds the rate of superflares of comparable energy on Sun-like stars [23] by orders of magnitude.

To monitor 47 Tuc, we consider the Wide Field Camera 3 instrument on the Hubble Space Telescope (HST), using the F225W filter. This instrument's field of view is sufficient to capture most of the DM core, and the UV filter alleviates stellar crowding [24]. In Fig. 1, we show the region where at least one event with SNR ≥ 5 is expected in one week of continuous observation. Since the event rate scales as $1/M_{\rm DM}$, new parameter space could be probed with as little as one hour of observation.

Discussion.—For concreteness, we have focused on specific assumptions and experimental searches, but our results also apply more generally. For instance, we have taken elastic scattering as a generic benchmark, but specific models can give rise to nonelastic interactions, such as catalyzing proton decay, annihilating with ordinary matter, or absorbing part of the dissipated energy. We have also assumed a geometric cross section for baryon scattering because it is the result of any sufficiently strong interaction that is not long-ranged, but the dark asteroid can be partly transparent to baryons, or interact by a long-range force, yielding a smaller or larger cross section respectively. These effects can be accounted for by simply scaling the energy deposited per length, $F_{\rm dr}$, as long as $R_0 \gtrsim R_{\rm DM}$.

The possibility of detecting dark asteroid impacts in nearby stars provides an interesting target for UV transient searches with small satellites [25, 26, 27], while more powerful instruments would be well-suited for focused searches. These observations are enabled by the rapid advance of time-domain astronomy, which we have shown provides an unusual route to discovering the nature of dark matter.

Acknowledgments
We thank Patrick Eggenberger, Rebecca Leane, Bruce Macintosh, Eric Mamajek, Georges Meynet, Payel Mukhopadhyay, Stephen Ro, Ningqiang Song, and Natalia Toro for helpful discussions. The authors were supported by the U.S. Department of Energy under contract number DE-AC02-76SF00515. SARE was also partially supported by SNF grant P400P2_186678. KZ is supported by the NSF GRFP under grant DGE-1656518.

References
[1] Jacobs D M, Starkman G D and Lynn B W 2015 *Mon. Not. Roy. Astron. Soc.* **450** 3418–3430 (*Preprint* 1410.2236)
[2] Burdin S, Fairbairn M, Mermod P, Milstead D, Pinfold J, Sloan T and Taylor W 2015 *Phys. Rept.* **582** 1–52 (*Preprint* 1410.1374)
[3] Bai Y, Long A J and Lu S 2020 *JCAP* **09** 044 (*Preprint* 2003.13182)
[4] Paxton B, Smolec R, Schwab J, Gautschy A, Bildsten L, Cantiello M, Dotter A, Farmer R, Goldberg J A, Jermyn A S, Kanbur S M, Marchant P, Thoul A, Townsend R H D, Wolf W M, Zhang M and Timmes F X 2019 *The Astrophysical Journal Supplement* **243** 10 (*Preprint* 1903.01426)
[5] Choi J, Dotter A, Conroy C, Cantiello M, Paxton B and Johnson B D 2016 *ApJ* **823** 102 (*Preprint* 1604.08592)
[6] Husser T O, Wende-von Berg S, Dreizler S, Homeier D, Reiners A, Barman T and Hauschildt P H 2013 *Astronomy & Astrophysics* **553** A6 (*Preprint* 1303.5632)
[7] ReVelle D O 1976 *Journal of Geophysical Research* **81** 1217–1230
[8] Pierce A D 2019 *Acoustics: an introduction to its physical principles and applications* (Springer)
[9] Dvorkin C, Blum K and Kamionkowski M 2014 *Phys. Rev. D* **89** 023519 (*Preprint* 1311.2937)
[10] Bhoonah A, Bramante J, Schon S and Song N 2020 (*Preprint* 2010.07240)
[11] Niikura H, Takada M, Yasuda N, Lupton R H, Sumi T, More S, Kurita T, Sugiyama S, More A, Oguri M and Chiba M 2019 *Nature Astronomy* **3** 524–534 (*Preprint* 1701.02151)
[12] Gould A 1987 *The Astrophysical Journal* **321** 571–585
[13] Sagiv I, Gal-Yam A, Ofek E O, Waxman E, Aharonson O, Kulkarni S R, Nakar E, Maoz D, Trakhtenbrot B, Phinney E S, Topaz J, Beichman C, Murthy J and Worden S P 2014 *The Astronomical Journal* **147** 79 (*Preprint* 1303.6194)
[14] Ivezić Ž, Kahn S M, Tyson J A, Abel B, Acosta E, Allsman R, Alonso D, AlSayyad Y, Anderson S F, Andrew J, Angel J R P, Angeli G Z, Ansari R, Antilogus P, Araujo C, Armstrong R, Arndt K T *et al.* 2019 *ApJ* **873** 111 (*Preprint* 0805.2366)
[15] Moore B 1996 *The Astrophysical Journal Letters* **461** L13
[16] Ibata R, Nipoti C, Sollima A, Bellazzini M, Chapman S and Dalessandro E 2013 *Mon. Not. Roy. Astron. Soc.* **428** 3648 (*Preprint* 1210.7787)
[17] Peebles P J E 1984 *Astrophys. J.* **277** 470–477
[18] Creasey P, Sales L V, Peng E W and Sameie O 2019 *Mon. Not. Roy. Astron. Soc.* **482** 219–230 (*Preprint* 1806.11118)
[19] Griffen B F, Drinkwater M J, Thomas P A, Helly J C and Pimbblet K A 2010 *MNRAS* **405** 375–386 (*Preprint* 0910.0310)
[20] Saitoh T R, Koda J, Okamoto T, Wada K and Habe A 2006 *Astrophys. J.* **640** 22–30 (*Preprint* astro-ph/0511692)
[21] Gao L, White S D M, Jenkins A, Stoehr F and Springel V 2004 *MNRAS* **355** 819–834 (*Preprint* astro-ph/0404589)
[22] Navarro J F, Frenk C S and White S D M 1996 *Astrophys. J.* **462** 563–575 (*Preprint* astro-ph/9508025)
[23] Okamoto S, Notsu Y, Maehara H, Namekata K, Honda S, Ikuta K, Nogami D and Shibata K 2021 *ApJ* **906** 72 (*Preprint* 2011.02117)
[24] Knigge C, Zurek D R, Shara M M and Long K S 2002 *ApJ* **579** 752–759 (*Preprint* astro-ph/0207060)
[25] Brosch N, Balabanov V and Behar E 2014 *Astrophysics and Space Science* **354** 205–209
[26] Mathew J, Ambily S, Prakash A, Sarpotdar M, Nirmal K, G Sreejith A, Safonova M, Murthy J and Brosch N 2018 *Experimental Astronomy* **45** 201–218 (*Preprint* 1801.10405)
[27] Serjeant S, Elvis M and Tinetti G 2020 *Nature Astronomy* **4** 1031–1038 (*Preprint* 2011.03478)